Science of the Total Environment 745 (2020) 141121

Contents lists available at ScienceDirect

Science of the Total Environment

journal homepage: www.elsevier.com/locate/scitotenv

Potential in paleoclimate reconstruction of modern pollen assemblages from natural and human-induced vegetation along the Heilongjiang River basin, NE China

Dongxue Han [a], Chuanyu Gao [a], Yunhui Li [a], Hanxiang Liu [b], Jinxin Cong [a], Xiaofei Yu [a,c], Guoping Wang [a,*]

[a] Key Laboratory of Wetland Ecology and Environment, Northeast Institute of Geography and Agroecology, Chinese Academy of Sciences, Changchun 130102, China
[b] Key Laboratory of Alpine Ecology, Institute of Tibetan Plateau Research, Chinese Academy of Sciences, Beijing 100101, China
[c] School of Environment, Northeast Normal University, Changchun 130117, China

HIGHLIGHTS

- Modern pollen assemblages can distinguish natural and human-induced vegetation.
- Pollen in human-induced vegetation types can be used to reconstruct past climate.
- The mean annual temperature mainly impacts modern pollen distribution in NE China.
- Pollen concentration could indicate human influence intensity.

GRAPHICAL ABSTRACT

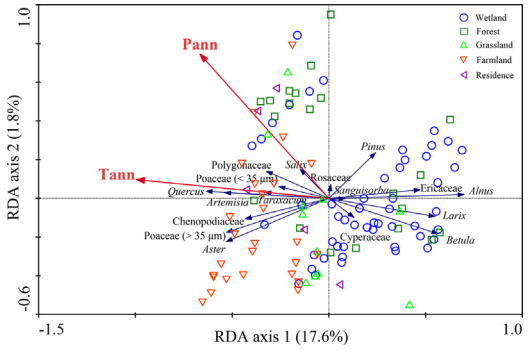

ARTICLE INFO

Article history:
Received 3 June 2020
Received in revised form 15 July 2020
Accepted 18 July 2020
Available online 22 July 2020

Editor: Fernando A.L. Pacheco

Keywords:
Heilongjiang River basin
High latitudes
Transfer function
Pollen-vegetation-climate
Human activities

ABSTRACT

The relationships among modern pollen, vegetation, climate and human activities can help improving the reliability of reconstruction of past vegetation, regional climate and human activities based on fossil pollen records. We used a dataset of 114 surface soil pollen samples from natural vegetation (wetlands, forests and grasslands) and human-induced vegetation (farmlands and residences) along the Heilongjiang River basin in northeast China to explore the relationships among modern pollen, vegetation, climate and human activities. The results indicated that surface pollen assemblages differentiated modern vegetation well in natural and human-induced vegetation types. The wetlands were mainly composed of Cyperaceae, along with *Artemisia*, weeds Poaceae (<35 μm) and *Sanguisorba*. The forests were predominated by *Pinus* and *Betula*. *Artemisia*, weeds Poaceae (<35 μm) and Chenopodiaceae were the most important pollen taxa in grasslands. The farmlands were characterized by *Artemisia*, *Aster*, Chenopodiaceae, cereal Poaceae (>35 μm) and *Taraxacum*. The pollen assemblages of residences were composed of weeds Poaceae (<35 μm), Chenopodiaceae and *Salix*. Ordination analyses based on main pollen taxa and climatic variables were used to determine the relationships between pollen and climate, suggesting the surface pollen assemblages were primarily influenced by the mean annual temperature (Tann) in northeast China. The statistical performance of transfer function between pollen and Tann were well indicating the modern pollen assemblages could be reliably used in paleoclimate reconstruction in our study area. Furthermore, human-induced vegetation had high frequencies of human-companion pollen taxa, such as Chenopodiaceae, *Aster*, *Taraxacum* and cereal Poaceae (>35 μm). Pollen concentrations of human-induced vegetation were lower than natural vegetation types, which could be used as an indicator of human influence intensity.

* Corresponding author.
E-mail address: wangguoping@neigae.ac.cn (G. Wang).

https://doi.org/10.1016/j.scitotenv.2020.141121
0048-9697/

1. Introduction

Fossil pollen evidences are one of the important proxy indicators of past vegetation and regional climate reconstruction (Qin et al., 2015; Wei and Zhao, 2016). Modern surface pollen data and its relationships with climatic factors are the basis for the accurate reconstruction of paleoclimate combined with fossil pollen records (Zhang et al., 2018; Huang et al., 2018). However, human activities are pervasive in most ecosystems which may bias the reconstruction of paleovegetation and paleoclimate (Li et al., 2014; Huang et al., 2018). Consequently, it is first necessary to elucidate the relationships of modern pollen, vegetation, climate and human activities for better improving the explanation of fossil pollen records and predicting the future environmental change.

In the past two decades, extensive studies have focused on modern pollen-vegetation-climate relationships, paleoclimate reconstruction, and human impacts on vegetation. These studies mainly concentrated on northwestern China (Luo et al., 2010; Qin et al., 2015; Huang et al., 2018), for instance, Xinjiang region (Wei and Zhao, 2016; Zhang et al., 2016), Tibetan Plateau (Lu et al., 2011; Wei et al., 2011; Ma et al., 2017; Zhang et al., 2018) and Alashan Plateau (Herzschuh et al., 2004), also including Loess Plateau in central-eastern China (Zhao et al., 2012). Even though several researches have been carried out on modern pollen in north China (Li et al., 2009; Xu et al., 2009, 2010; Zhang et al., 2010), such as the eastern and the western part of northeast China (Geng et al., 2019; Cui et al., 2019) and Changbai Mountains (Sun et al., 2003; Xu et al., 2007), which are primarily concentrated on forest and steppe areas. The modern pollen studies of human influences on vegetation are either scarce in northeast China (Zhang et al., 2010; Li et al., 2012, 2015). The relationships among modern pollen, vegetation, climate and human activities at a relatively broad scale in high latitude region of northeast China are still poorly investigated, which hampered the better interpretation of fossil pollen records and the reliably quantitative reconstruction of paleoclimate in this region.

The Heilongjiang River basin in northeast China is extremely sensitive to global climate change due to its unique geographical position, which situated in the north margin of the East Asian monsoon region. The climate is controlled by both the East Asian monsoon and the westerly winds in the region (Gao et al., 2018a; Han et al., 2019). In the context of global warming, the Heilongjiang River basin which located in high-latitude region currently experience an amplified warming than other regions in the world (Melles et al., 2019; Liu et al., 2019). The Heilongjiang River basin is also situated in the transition zone between the eastern edge of temperate grassland and the southern margin of boreal forest in Eurasia, and it is the primary distribution area of wetlands, nearly 42,450 km^2 of peatlands are distributed in the Greater Khingan Mountains, 13,190 km^2 in the Lesser Khingan Mountains, and 10,520 km^2 in the Sanjiang Plain (Xing et al., 2015). Peats are regarded as one of the faithful geological archives of past vegetation and climate change, which reliably register peatland development process and regional climatic variation, and have a great potential for paleovegetation and paleoclimate reconstruction. While, large-scale land reclamation has resulted in nearly 80% native wetlands being converted to cultivated areas in the Sanjiang Plain since the 1950s (Xing et al., 2016; Gao et al., 2018b; Liu et al., 2018). The Heilongjiang River basin provides an ideal area to investigate the modern pollen assemblages in natural and human-induced vegetation. Thus, an understanding of modern pollen, vegetation, climate and human activities relationships is necessary which can provide valuable implications for the reconstruction of historical vegetation and regional climate change in northeast China.

In the current study, we collected 114 surface soil pollen samples from natural vegetation types (wetlands, forests and grasslands) and human-induced vegetation (farmlands and residences) along the Heilongjiang River basin in northeast China, from which we identified 43 pollen taxa. The aims of this paper were (1) to explore the modern pollen assemblages characteristics of natural and human-induced vegetation types; (2) to evaluate the relationships between modern surface pollen assemblages and climatic variables and to determine the most crucial factor controlling the modern pollen assemblages; (3) to examine the pollen-climate calibration model performance and to furtherly provide a reference for past vegetation and climate reconstruction based on fossil pollen records in northeast China.

2. Materials and methods

2.1. Study area and sampling

The study area (45.29°–53.50° N, 121.51°–134.15° E) is located in the south of the Heilongjiang River basin in northeast China, including Greater Khingan Mountains, Lesser Khingan Mountains and Sanjiang Plain (Fig. 1). The topography of the basin is generally high in the west and low in the east. The west of the basin is mainly mountains, the east part of the basin is dominated by plains. The elevation of sampling sites ranges between 42 m and 932 m above sea level. The Heilongjiang River basin is the northernmost edge of the global monsoon climate zone, belongs to a temperate continental monsoon climate. The mean annual temperature (Tann) here ranges between −8 and 6 °C, the average temperature in January is about −28.5 °C, winter is long, dry and cold from November to April. The average temperature in July is about 19.5 °C, summer is short, wet and hot between June and August. The mean annual precipitation (Pann) amounts to 250–800 mm (decreased gradually from the east to the west), more than 80% of the rainfall occurs between May and September.

The sampling sites were selected at intervals of average 30 km along the Heilongjiang River basin in Heilongjiang Province, northeast China. A total of 114 surface soil samples from natural vegetation types (including 51 wetlands, 21 forests and 11 grasslands) and human-induced vegetation (including 26 farmlands and 5 residences) were collected in July 2017 (Fig. 1). Samples were collected from 0 to 1 cm deep surface soil, to reduce sampling error, 5 points within a 3 m × 3 m sampling plot were mixed together. Longitude, latitude and altitude were recorded by GPS at each sampling site (Table S1). All samples were packed into tagged sealed polyethylene plastic bags, subsequently taken back to the laboratory for storage at −20 °C prior to analysis.

2.2. Pollen analysis

Pollen pre-treatment followed the conventional HCl-NaOH-HF methods (Fægri and Iversen, 1989), the preparation of pollen samples (1 g fresh sample) in the laboratory involved treatments with hydrochloric acid (HCl, 36%, 5 ml), sodium hydroxide (NaOH, 10%, 5 ml), hydrofluoric acid (HF, 40%, 5 ml), a 9:1 mixture (3 ml) of acetic anhydride and concentrated sulfuric acid, sieving with a 10-μm mesh screen in ultrasonic bath, and mounting in glycerine. At the beginning of the chemical processing, a tablet of *Lycopodium* spore (27,560 grains spores) was added to per sample for calculating absolute pollen concentrations (grains/g). Pollen was identified and counted using a light microscope (Olympus BX-53) at 400 times magnification, with the aid of published pollen atlases by Wang et al. (1995) and Tang et al. (2016). A reference of modern pollen from plants which collected in the study area also used. We identified and counted more than 400 terrestrial pollen grains (from a minimum of 3–4 slides) of each sample. The total sum of terrestrial pollen species was used for pollen percentages calculations (Zhao et al., 2010). We drew the diagrams of pollen assemblages using the Tilia software (version 1.7.16).

2.3. Numerical analyses

Ordination analyses were applied to investigate the relationships between pollen assemblages and environment variables using Canoco Software 4.5 (Ter Braak and Smilauer, 2003). To reduce the bias owing to the presence of rare pollen taxa, we selected 17 pollen taxa (percentage > 5%, occurred in at least 3 samples) for numerical analyses. Pollen

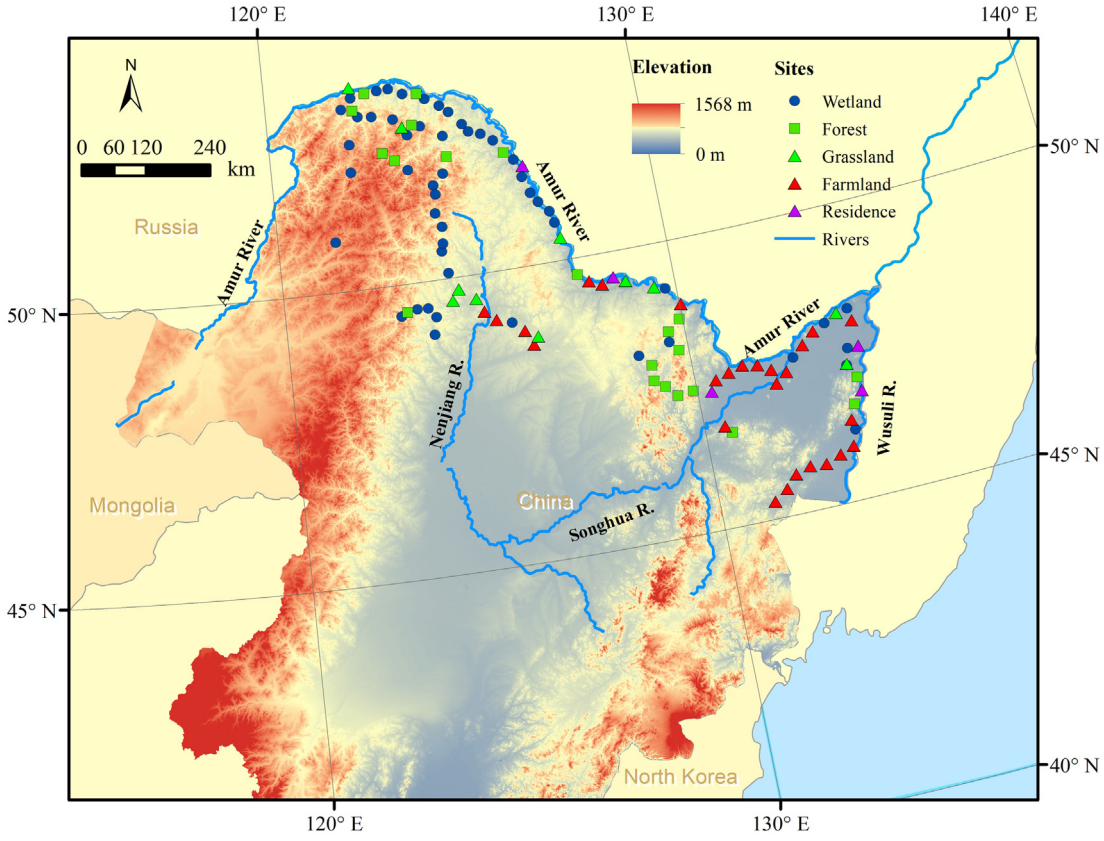

Fig. 1. Location of 114 surface pollen sampling sites from natural and human-induced vegetation types along the Heilongjiang River basin in northeast China.

percentages data of each sample was transformed into square root. Detrended correspondence analysis (DCA) was used to determine whether linear or unimodal based techniques should be employed in the subsequent ordination analysis. The gradient length of the first axis in DCA was 1.907 (less than 2), showing a linear structure of data set and suggesting the use of linear-based principal component analysis (PCA) and redundancy analysis (RDA).

The weighted averaging partial least squares (WA-PLS) (Ter Braak and Juggins, 1993) was selected to establish the transfer function between modern pollen community composition and environmental variable using R (R Core team, 2015) package rioja 0.9–9 (Juggins, 2016). Modern site-specific climate data was extracted from the WorldClim dataset with a spatial resolution of 1-km (Fick and Hijmans, 2017). Two key climate parameters (Tann and Pann) were used in this study. The pollen abundances were standardized and transformed into their square roots (28 pollen taxa were collected, minimum percentage > 1%, occurrences > 3 times). The selected 28 pollen taxa were *Picea*, *Abies*, *Larix*, *Pinus*, *Betula*, *Alnus*, *Quercus*, *Juglans*, *Salix*, *Ulmus*, Ericaceae, *Artimisia*, *Aster*, *Taraxacum*, Chenopodiaceae, Cyperaceae, *Thalictrum*, *Sanguisorba*, *Typha*, Polygonaceae, Ranunculaceae, Cruciferae, Umbelliferae, Leguminosae, Rosaceae, Compositae, Poaceae (<35 μm) and Poaceae (>35 μm). The statistical testing was performed using jack-knife method with cross-validation (Dixit et al., 1993). The evaluation of transfer function based on root-mean-square error of prediction (RMSEP), coefficient of determination (R^2) between observed and predicted values, and the maximum bias in residuals.

3. Results

3.1. Modern pollen assemblages

In total, 43 pollen taxa were identified in the 114 surface soil samples from natural and human-induced vegetation types, including 12 trees, 3 shrubs and 28 herbs. Arboreal trees were mainly consisted of *Pinus*, *Larix*, *Betula*, *Alnus*, *Quercus* and *Salix*, shrubs were mainly from Ericaceae and Rosaceae, herbs were dominated by Cyperaceae, *Sanguisorba*, Compositae, Chenopodiaceae, Poaceae and Polygonaceae (Fig. 2).

In wetlands, the contents of herbs were 4.5–90.8%, average 39.2%. The contents of trees and shrubs ranged from 9.3% to 95.5%, average 61.1%. Cyperaceae (average 17.9%) was the dominant pollen type, and the contents of *Artemisia* (average 8.7%), weeds Poaceae (<35 μm) (average 5.2%), Chenopodiaceae (average 2.5%) and *Sanguisorba* (average 1.1%) were also relatively higher. Tree pollen types were mainly *Betula* (average 35.7%), *Pinus* (average 10.7%), *Alnus* (average 4.7%), *Larix* (average 4.0%), *Quercus* (average 2.2%) and *Salix* (average 1.3%). The shrubs were consisted of Rosaceae (average 0.9%) and Ericaceae (average 0.7%). The altitudes of wetlands were 42–776 m, the ratios of arborous to non-arborous pollen (AP/NAP) were 0.1–18.6 (average 4.2), pollen concentration ranged from 6.6×10^3 to 4.0×10^5 grains/g (average 0.7×10^5 grains/g) (Fig. 3).

In forests, the percentages of arborous trees were 27.4–96.5%, average 72.5%, tree pollens were predominated by *Pinus* (average 28.6%), *Betula* (average 27.2%), *Alnus* (average 6.6%), *Larix* (average 2.7%), *Quercus* (average 2.4%) and *Salix* (average 1.4%). Shrub pollen percentage was about 2.5%, mainly Rosaceae (average 2.0%). Herbs were dominated by *Artemisia* (average 14.4%), weeds Poaceae (<35 μm) (average 3.6%), Chenopodiaceae (average 2.4%) and *Taraxacum* (average 1.0%). The altitudes of forests were 100–932 m, the AP/NAP was 0.4–27.6 (average 5.7), pollen concentration ranged from 4.4×10^3 to 2.4×10^5 grains/g (average 0.5×10^5 grains/g).

In grasslands, herbs percentages ranged from 11.2% to 84.4%, average 52.6%, mainly composed of *Artemisia* (average 27.9%), and relatively higher Cyperaceae (average 6.1%), weeds Poaceae (<35 μm) (average 6.0%), Chenopodiaceae (average 5.6%) and *Thalictrum* (average 1.4%). Tree pollen were mainly consisted of *Betula* (average 21.5%), *Pinus*

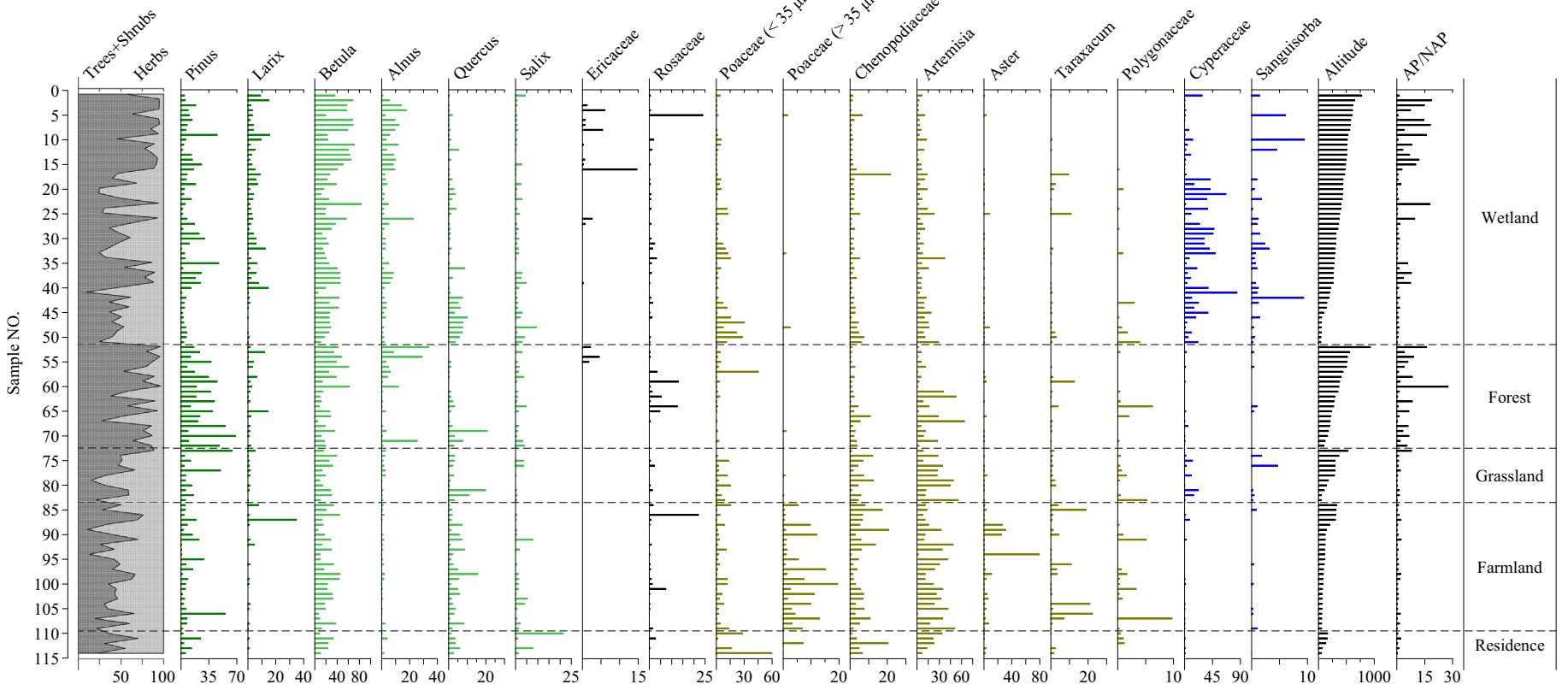

Fig. 2. Pollen percentage diagrams of 114 surface soil samples (51 wetlands, 21 forests, 11 grasslands, 26 farmlands and 5 residences). Only the main taxa were shown.

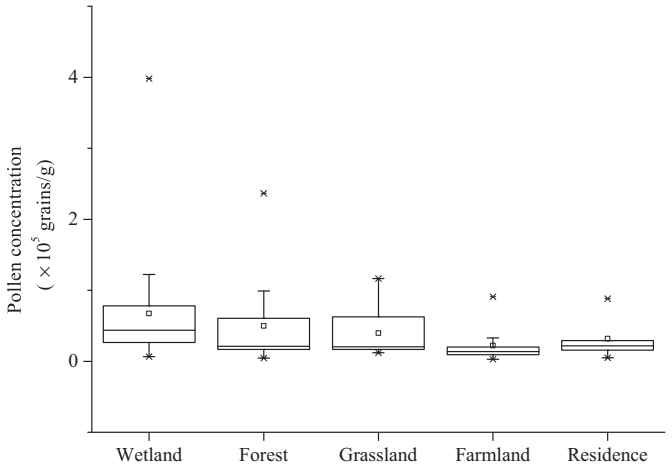

Fig. 3. Boxplots of pollen concentration in different vegetation types.

(average 17.0%), *Quercus* (average 4.2%), *Alnus* (average 1.4%) and *Larix* (average 1.2%). The altitudes of grasslands were 48–531 m, the AP/NAP was 0.2–7.9 (average 1.5), pollen concentration ranged from 1.2×10^4 to 1.2×10^5 grains/g (average 0.4×10^5 grains/g).

In farmlands, herb pollen percentages were 24.0–89.2%, average 56.8%, mainly consisted of *Artemisia* (average 23.1%), *Aster* (average 8.2%), Chenopodiaceae (average 6.2%), cereal Poaceae (>35 μm) (average 5.4%), weeds Poaceae (<35 μm) (average 4.7%), *Taraxacum* (average 4.0%) and Compositae (average 1.2%). The average percentage of tree pollen was 41.7%, dominated by *Betula* (average 22.6%), *Pinus* (average 9.5%), *Quercus* (average 3.9%) and *Salix* (average 1.2%). The altitudes of farmlands were 57–324 m, the AP/NAP was 0.1–2.4 (average 0.9), pollen concentration ranged from 2.8×10^3 to 9.1×10^4 grains/g (average 0.2×10^5 grains/g).

In residences, herbs percentages were 30.1–77.6%, average 57.2%, mainly composed of weeds Poaceae (<35 μm) (average 21.2%), *Artemisia* (average 19.7%), Chenopodiaceae (average 7.3%), Geraniaceae (average 3.4%), cereal Poaceae (>35 μm) (average 1.4%) and *Aster* (average 1.1%). the percentage of arborous trees is 48.0%, tree pollens are predominated by *Betula* (average 19.9%), *Pinus* (average 10.0%), *Salix* (average 6.3%) and *Quercus* (average 3.4%). The altitudes of residences were 54–166 m, the AP/NAP was 0.3–2.0 (average 0.9), pollen concentration ranged from 5.0×10^3 to 8.8×10^4 grains/g (average 0.3×10^5 grains/g).

3.2. Ordination analyses results

The gradient length of the first axis in DCA based on 17 selected main pollen taxa (minimum percentage > 5%, occurrences > 3 times) was 1.907 (less than 2), showing a linear structure of data set. The linear-based PCA results were shown in Fig. 4, the first axis and the second axis explained 26.6% and 22.3%, respectively, altogether accounted for 48.9% of the total variance in the pollen assemblages. The 114 surface soil pollen samples from natural (wetlands, forests and grasslands) and human-induced (farmlands and residences) vegetation types were significant different in pollen assemblages and clustered obviously in the PCA ordination diagram. The PCA axis 1 separated the cold-tolerant *Larix* and *Pinus* on the left from the thermophilic *Quercus* on the right. The PCA axis 1 can represent the temperature changes: positive and negative values indicated warm and cold conditions, respectively. The PCA axis 2 separated the hygrophilic Cyperaceae and *Sanguisorba* above from drought-tolerant Ericaceae below. The PCA axis 2 mainly represented effective moisture changes: positive values indicated wet condition, while negative values implied dry environment.

To better understand the relationship between pollen assemblages and environment in natural and human-induced vegetation types in

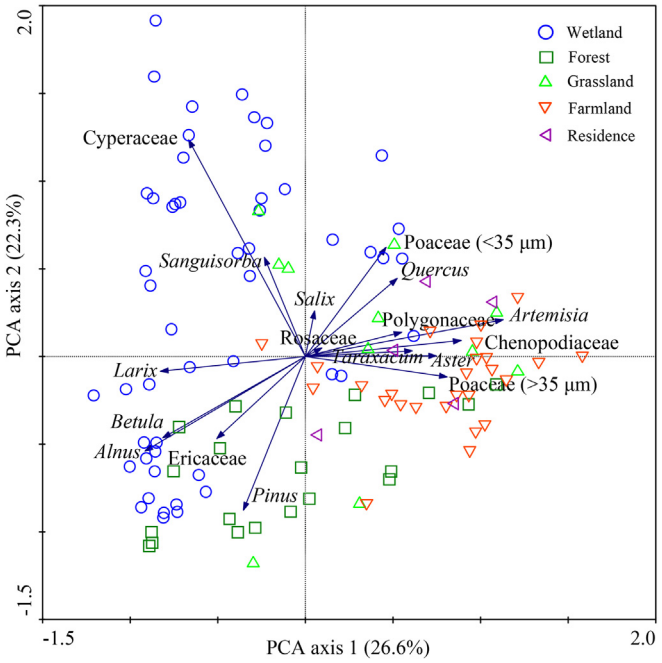

Fig. 4. PCA ordination of principal 17 pollen taxa and 114 surface soil samples.

northeast China, Tann and Pann were selected as the major environmental variables, and 17 main pollen taxa (the same as in the DCA and PCA) represented the pollen assemblages. The linear model RDA was selected based on DCA, the RDA results implied that Tann and Pann captured 17% and 2% of the total variance in the pollen distributions, respectively (Fig. 5). The Tann was the main driving factor that influenced the surface pollen assemblages in our study region, consequently, we constructed the transfer function between modern pollen assemblages and Tann. *Quercus*, *Artemisia*, Chenopodiaceae, cereal Poaceae (>35 μm) and *Aster* were positively correlated with Tann, whereas *Larix*, *Betula*, *Alnus*, *Pinus*, Ericaceae and Cyperaceae were negatively correlated with Tann.

3.3. Construction of calibration model

Based on ordination analyses, the WA-PLS calibration model was applied to establish quantitative relationship between modern surface soil pollen and Tann. A total of 28 pollen taxa were selected (minimum percentage > 1%, occurrences > 3 times). We used different numbers of surface soil samples to constructed transfer functions, such as using all sampled vegetation types (114 sites, wetlands/forests/grasslands/

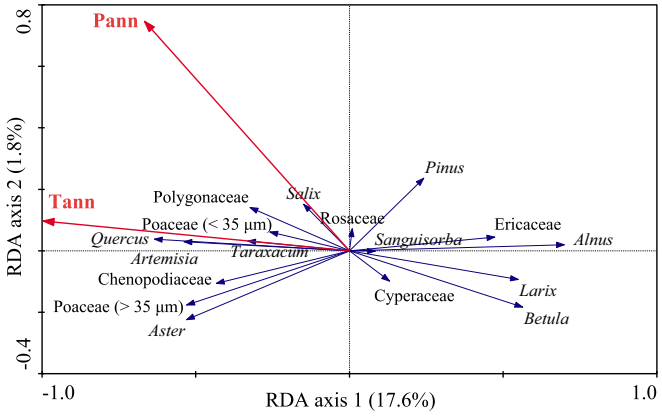

Fig. 5. Biplots of redundancy analysis (RDA) results.

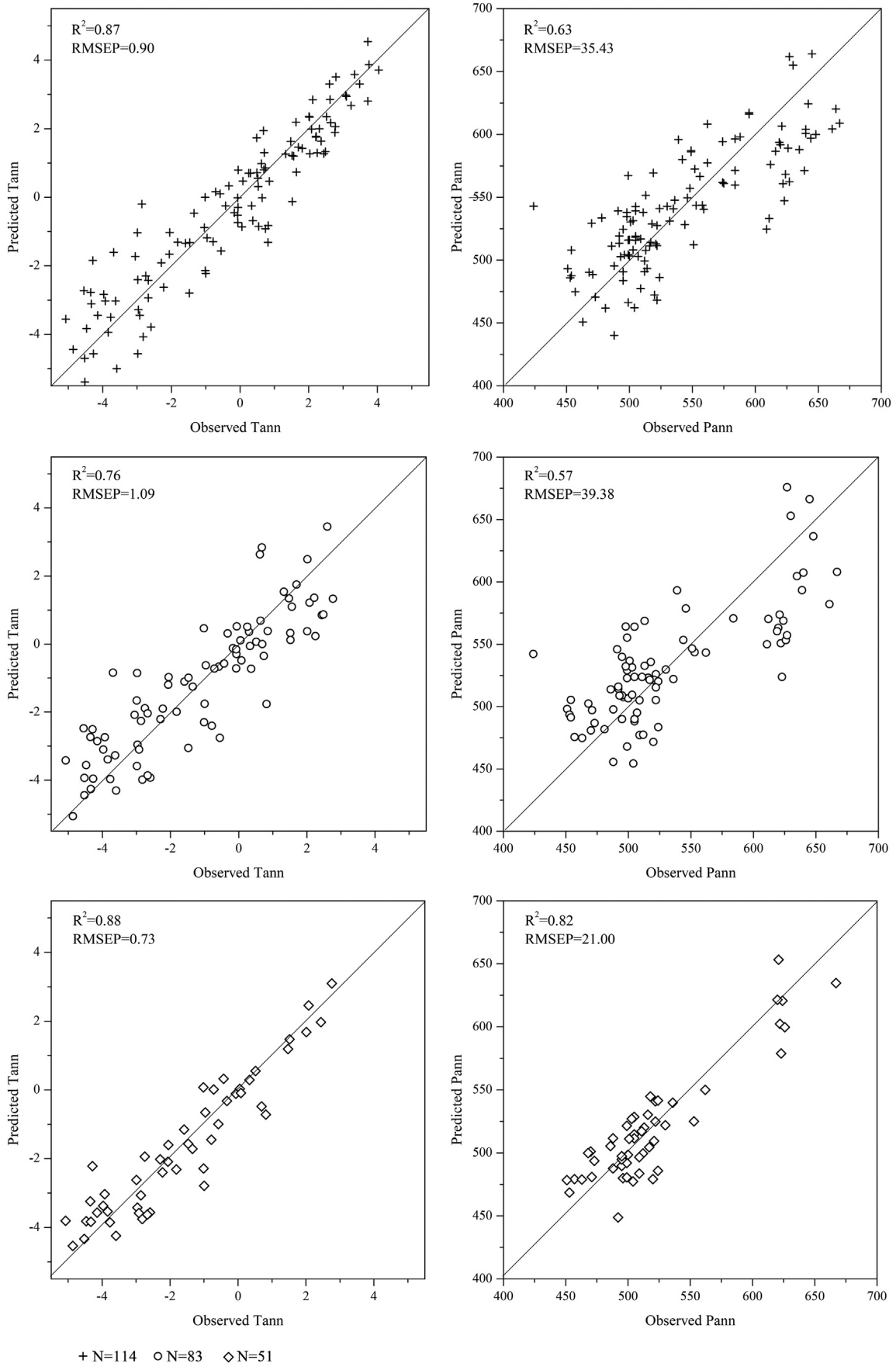

Fig. 6. Scatter plots of observed Tann (Pann) versus WA-PLS predicted Tann (Pann) values based on the surface soil samples. Cross represents 114 samples, circle represents 83 samples, and diamond represents 51 samples.

farmlands/residences), employing natural vegetation types except for human-induced types (83 sites, wetlands/forests/grasslands), and applying just one vegetation type (51 sites, wetlands). The statistical performance was better with higher R^2 and lower RMSEP and maximum bias. The five-component WA-PLS model was selected which displayed the best performance (the highest value of R^2 and the lowest value of RMSEP) for reconstruction of Tann (Table S2). There was a better statistical performance ($R^2 = 0.87$, RMSEP = 0.90, maximum bias = 0.83) when using all 114 samples to construct the WA-PLS calibration model between modern pollen and Tann (Fig. 6). Though the calibration model based on 51 wetland sites had the highest R^2 (0.88) and the lowest RMSEP (0.73), the number of sample sites was less than half of all 114 sites, additionally, it had a higher maximum bias (0.89).

4. Discussion

4.1. Variation of pollen assemblages in natural and human-induced vegetation types

There were obvious discrepancies of main pollen taxa and percentages in natural and human-induced vegetation types along the Heilongjiang River basin in northeast China (Fig. 2). The most remarkable characteristic in the wetlands was the highest contents of Cyperaceae and *Sanguisorba* as the predominant species was *Carex* in most of the wetland types. There were also relatively higher contents of Poaceae (<35 μm) as the dominant plants were *Phragmites communis* or *Calamagrostis angustifolia* in some wetlands. Besides, the percentages of *Larix* (4.2%) in the wetlands were also the highest in all the vegetation types, due to the presence of *Larix gmelinii* forests in the Greater Khingan Mountains (Li et al., 2015). The *Larix* pollen content was low though in *Larix* woodlands because of its lower pollen production and poorer dispersal distance (Ma et al., 2008; Li et al., 2015). The percentage of arboreous pollen was higher (more than 60%) and the average AP/NAP was 4.2 (Fig. 2), owing to the sampling sites of wetlands in our study were almost located in the Greater Khingan Mountains where the altitudes were relatively higher than the Lesser Khingan Mountains and the Sanjiang Plains along the Heilongjiang River basin.

Forests were primarily characterized by *Pinus*, *Betula*, *Alnus*, *Larix*, *Quercus* and *Salix*, the percentages of *Pinus* (28.6%), *Betula* (27.2%) and *Alnus* (6.6%) were higher than other vegetation types (except the content of *Betula* was a little lower than wetlands). The common plants in undergrowth were shrubs (Rosaceae) and herbs (mainly *Artemisia*, weeds Poaceae and Chenopodiaceae). The sampling sites of forests were situated in the mountains with higher altitudes, the arboreous pollen content in the forests was the highest which exceeded 70%, additionally, the AP/NAP was the highest (average up to 5.7) among all the vegetation types (Fig. 2). Cui et al. (2019) analyzed the pollen assemblages characteristics of the forests in the western part of northeast China, they demonstrated the forests were predominated by *Betula*, *Alnus*, *Larix* and *Pinus*, and the tree pollen percentages were more than 70% as well. Zhang et al. (2010) also suggested the forests were characterized by *Pinus* and *Betula* in northeast China, the proportion of tree pollen was average 76%, besides, *Artemisia* and Chenopodiaceae accounted for 13.9% and 2.3% respectively in forest zone.

The herbaceous pollen content (more than 50%) in grasslands was higher than wetlands and forests, the average AP/NAP was 1.5, the herbs pollen content gradually increased and trees pollen content gradually decreased with the reduction of altitude. Li et al. (2015) also indicated that the herb pollen taxa increased and tree pollen taxa reduced as the increasing distance to the mountains. The content of *Artemisia* (up to 30%) was the highest in grasslands compared with other vegetation types. In addition, the contents of Chenopodiaceae and weeds Poaceae (<35 μm) were relatively higher than wetlands and forests. Cui et al. (2019) also suggested the steppe was characterized by *Artemisia* and Chenopodiaceae in northeast China.

Farmlands were predominated by *Artemisia*, *Aster*, Chenopodiaceae, cereal Poaceae (>35 μm) and *Taraxacum*, along with weeds Poaceae (<35 μm) and Polygonaceae. Compared with the grasslands, there were higher contents of human-companion pollen in the farmlands, such as *Aster*, *Taraxacum* and Chenopodiaceae. The contents of cereal Poaceae (>35 μm) could up to 20% in several farmlands, and the cereal Poaceae (>35 μm) percentages exhibited an increasing trend with the decrease of altitude. The Sanjiang Plain was more fertile and suitable for human occupation and agricultural activities than the mountains. Li et al. (2012) also demonstrated the contents of cereal Poaceae and Cruciferae were lower over elevation. The relatively lower proportions of *Pinus* (close to 10%) might because the farmlands were derived from lower altitude plains where was short of pine trees than the mountains, and the *Pinus* pollen was mainly from long-distance transportation by wind (Li et al., 2015). The content of *Pinus* pollen gradually reduced as the increasing distance to the mountains.

Residences were characterized by the highest proportions of weeds Poaceae (<35 μm), Chenopodiaceae and *Salix*, along with cereal Poaceae (>35 μm) and *Aster*. There were higher weeds Poaceae (<35 μm) and lower cereal Poaceae (>35 μm) in the residences compared with the farmlands. The highest percentages of *Salix* (6.3%) owing to the planted willow trees on both sides of roads in the residential areas. The herbaceous pollen percentages were the highest in all the vegetation types, and the AP/NAP was the lowest (Fig. 2, less than 1, similar to the farmlands).

4.2. Potential of natural and human-induced vegetation in paleoclimate reconstruction

Cui et al. (2019) used 44 surface soil pollen samples (forest, meadow and steppe) to explore relationships of pollen, vegetation and climate. There existed significant correlations between pollen assemblages and the mean annual temperature and then the mean annual precipitation based on RDA analysis, they suggested pollen assemblages could indicate the variation of temperature and precipitation in the western part of northeast China. Geng et al. (2019) applied 43 surface pollen samples of forests (conifer forest, broadleaved forest and mixed forest), they also concluded pollen assemblages could reflect regional temperature change in the eastern part of northeast China.

In our study, PCA analysis based on 17 main pollen taxa from 114 surface soil pollen samples (wetlands, forests, grasslands, farmlands and residences) marked there were obvious discrepancies of pollen assemblages from natural and human-induced vegetation types which were distributed along temperature and precipitation gradients (Fig. 4). RDA analysis indicated the Tann was the most important influencing driver in variation of pollen assemblages along the Heilongjiang River basin in northeast China (Fig. 5). Based on ordination analyses and WA-PLS model, we selected different vegetation types to construct the calibration models between Tann and pollen assemblages to evaluate a better transfer function applied in paleoclimate reconstruction. As we could see in Fig. 6, it presented a better statistical performance when using all the five different vegetation types (114 sites), including both the natural and human-induced vegetation types. Li et al. (2012) implied the pollen assemblages from human-induced vegetation types could reflect regional climate well in northeast China. Xu et al. (2010) found modern pollen samples with serious human influence had no obvious impact on the overall results of paleoclimate reconstruction in north China. Huang et al. (2018) also demonstrated modern pollen spectra of human-induced vegetation could potentially be used for quantitative reconstruction of past climate in arid China. The pollen assemblages from natural and human-induced vegetation types in our study region (along the Heilongjiang River basin in northeast China) did reliably reflect the variation of vegetation and could be used in the reconstruction of paleoclimate.

4.3. Indications of anthropogenic activities

The sampling sites of natural vegetation types (wetlands, forests and grasslands) were mainly located in the Greater and Lesser Khingan Mountains where the elevation was higher than the plains. The human-induced vegetation types (farmlands and residences) were almost situated in the Sanjiang Plain with lower elevation. In the wetlands and forests, the contents of tree pollen accounted for more than 60%, whereas the herb pollen contents exceeded 55% in the farmlands and residences (Fig. 2). And the content of cereal Poaceae (>35 μm) were the highest in the farmlands among all the vegetation types along Heilongjiang River basin in northeast China. Variations in the contents of arboreous and cereal Poaceae (>35 μm) pollen are commonly considered as the most directly evidence of human disturbance (Li et al., 2015). Human beings cleared vegetation (e.g., felled trees) and developed lands (e.g., planted crops) to meet their daily needs when migrated to a new area. Li et al. (2012) compared the pollen assemblages of farmlands from different elevation in northern China, they had found tree pollen proportions increased while cereal declined with the increase of altitude, indicating declined human impact. Likewise, the increased cereal Poaceae (>35 μm) and the decreased arboreal pollen with the reduction of altitude in our study region revealed the intensified human activities with the declined altitude.

Besides, the increasing of pollen indicators of human activities, including *Artemisia*, Chenopodiaceae, weeds Poaceae (<35 μm), Polygonaceae, *Taraxacum*, *Aster* and other Compositae species, also suggested the intensified anthropogenic activities (Zhang et al., 2015; Li et al., 2015). In the farmlands, the pollen was primarily dominated by *Artemisia*, along with *Aster*, Chenopodiaceae, cereal Poaceae (>35 μm), weeds Poaceae (<35 μm) and *Taraxacum*, the residences were mainly characterized by weeds Poaceae (<35 μm), *Artemisia* and Chenopodiaceae (Fig. 2). The higher levels of human-companion pollen contents in human-disturbed vegetation types reflected strengthened human disturbance compared with the natural vegetation types.

Furthermore, the pollen concentration was the highest in the wetlands (average 0.7×10^5 grains/g), the pollen concentration of natural vegetation (forests, 0.5×10^5 grains/g; grasslands, 0.4×10^5 grains/g) were higher than the human-disturbed vegetation types (farmlands, 0.2×10^5 grains/g; residences, 0.3×10^5 grains/g) (Fig. 3). Li et al. (2012) revealed total pollen concentrations of farmlands were obviously lower than wastelands and natural vegetation types, human activities were the main reason which resulted in low pollen concentration in the farmlands. Pollen concentration could be regarded as an indicator of human influence intensity to some degree, intensified human impact caused the reduction of pollen concentration.

5. Conclusions

(1) Modern pollen assemblages clearly distinguished the natural and human-induced vegetation types along the Heilongjiang River basin from the northeast China. Modern pollen spectra and PCA results exhibited that different vegetation types were characterized by distinctive pollen assemblages. Wetlands were principally characterized by Cyperaceae and *Sanguisorba*. Forests were dominated by arboreous pollen, mainly *Pinus* and *Betula*. The content of *Artemisia* was the highest in grasslands. Farmlands were primarily consisted of *Artemisia*, *Aster*, Chenopodiaceae, cereal Poaceae (>35 μm) and *Taraxacum*. Residences were mainly composed of weeds Poaceae (<35 μm), Chenopodiaceae and *Salix*.

(2) The correlation of modern pollen assemblages and climate parameters based on RDA analysis suggested that the mean annual temperature was the dominant factor controlling the variations in distribution of modern pollen along the Heilongjiang River basin in northeast China. The WA-PLS calibration model between modern pollen assemblages and the mean annual temperature presented a well statistical performance and could be used to reconstruct the temperature in this region.

(3) AP/NAP was the highest in forests, the arboreous trees content declined with the decrease of altitude. However, the proportion of human-companion plants, such as *Artemisia*, *Aster*, *Taraxacum*, Chenopodiaceae, weeds Poaceae (<35 μm) and cereal Poaceae (>35 μm) increased with the decrease of altitude, indicating intensified human activities. Moreover, pollen concentrations were lower in human-induced vegetation (farmlands and residences) than natural vegetation types (wetlands, forests and grasslands), which also could be used to indicate the intensity of human disturbance.

Supplementary data to this article can be found online at https://doi.org/10.1016/j.scitotenv.2020.141121.

CRediT authorship contribution statement

Dongxue Han: Writing - original draft, Data curation. **Chuanyu Gao:** Validation, Software. **Yunhui Li:** Investigation, Methodology. **Hanxiang Liu:** Investigation, Formal analysis. **Jinxin Cong:** Software, Data curation. **Xiaofei Yu:** Visualization, Supervision. **Guoping Wang:** Conceptualization, Writing - review & editing.

Declaration of competing interest

The authors declare that they have no known competing financial interests or personal relationships that could have appeared to influence the work reported in this paper.

Acknowledgements

The authors gratefully acknowledge the assistance of the Analysis and Test Center of the Northeast Institute of Geography and Agroecology of the Chinese Academy of Sciences. We also thank Fernando A.L. Pacheco and two anonymous reviewers for their constructive comments and suggestions to improve the quality of this manuscript. This work was supported by the National Key Research and Development Project [grant number 2016YFA0602301]; the National Natural Science Foundation of China [grant numbers 41701217, 41911530188, 41571191]; the Youth Innovation Promotion Association CAS [grant number 2020235]; the Fundamental Research Funds for the Central Universities [grant number 2412019BJ003]; the Jilin Provincial Department of Science and Technology [grant number 20190101011JH].

References

Core Team, R, 2015. R: A Language and Environment for Statistical Computing. R Foundation for Statistical Computing, Vienna, Austria.

Cui, Q.Y., Zhao, Y., Qin, F., Liang, C., Li, Q., Geng, R.W., 2019. Characteristics of the modern pollen assemblages from different vegetation zones in Northeast China: implications for pollen-based climate reconstruction. Sci. China Earth Sci. 62, 1564–1577. https://doi.org/10.1007/s11430-018-9386-9.

Dixit, S.S., Cumming, B.F., Birks, H.J.B., Smol, J.P., Kingston, J.C., Uutala, A.J., Charles, D.F., Camburn, K.E., 1993. Diatom assemblages from Adirondack lakes (New York, USA) and the development of inference models for retrospective environmental assessment. J. Paleolimnol. 8, 27–47. https://doi.org/10.1007/BF00210056.

Fægri, K., Iversen, J., 1989. Textbook of Pollen Analysis. 4th ed. John Wiley and Sons, London, UK.

Fick, S.E., Hijmans, R.J., 2017. Worldclim 2: new 1-km spatial resolution climate surfaces for global land areas. Int. J. Climatol. 37, 4302–4315. https://doi.org/10.1002/joc.5086.

Gao, C.Y., He, J.B., Zhang, Y., Cong, J.X., Han, D.X., Wang, G.P., 2018a. Fire history and climate characteristics during the last millennium of the Great Hinggan Mountains at the monsoon margin in northeastern China. Glob. Planet. Chang. 162, 313–320. https://doi.org/10.1016/j.gloplacha.2018.01.021.

Gao, C.Y., Zhang, S.Q., Liu, H.X., Cong, J.X., Li, Y.H., Wang, G.P., 2018b. The impacts of land reclamation on the accumulation of key elements in wetland ecosystems in the Sanjiang Plain, northeast China. Environ. Pollut. 237, 487–498. https://doi.org/10.1016/j.envpol.2018.02.075.

Geng, R.W., Zhao, Y., Cui, Q.Y., Qin, F., 2019. Representation of modern pollen assemblages with respect to vegetation and climate in Northeast China. Quat. Int. 532, 126–137. https://doi.org/10.1016/j.quaint.2019.11.003.

Han, D.X., Gao, C.Y., Yu, Z.C., Yu, X.F., Li, Y.H., Cong, J.X., Wang, G.P., 2019. Late Holocene vegetation and climate changes in the Great Hinggan Mountains, northeast China. Quat. Int. 532, 138–145. https://doi.org/10.1016/j.quaint.2019.11.017.

Herzschuh, U., Tarasov, P., Wünnemann, B., Hartmann, K., 2004. Holocene vegetation and climate of the Alashan Plateau, NW China, reconstructed from pollen data. Palaeogeogr. Palaeoclimatol. Palaeoecol. 211, 1–17. https://doi.org/10.1016/j.palaeo.2004.04.001.

Huang, X.Z., Chen, X.M., Du, X., 2018. Modern pollen assemblages from human-influenced vegetation in northwestern China and their relationship with vegetation and climate. Veg. Hist. Archaeobot. 27, 767–780. https://doi.org/10.1007/s00334-018-0672-0.

Juggins, S., 2016. Rioja: analysis of quaternary science data. R package version (0.9-9). http://cran.

Li, Y.C., Xu, Q.H., Zhang, L.Y., Wang, X.L., Cao, X.Y., Yang, X.L., 2009. Modern pollen assemblages of the forest communities and their relationships with vegetation and climate in northern China. J. Geogr. Sci. 19, 643–659. https://doi.org/10.1007/s11442-009-0643-6.

Li, M.Y., Li, Y.C., Xu, Q.H., Pang, R.M., Ding, W., Zhang, S.R., He, Z.G., 2012. Surface pollen assemblages of human-disturbed vegetation and their relationship with vegetation and climate in Northeast China. Chin. Sci. Bull. 57, 535–547. https://doi.org/10.1007/s11434-011-4853-9.

Li, J.Y., Zhao, Y., Xu, Q.H., Zheng, Z., Lu, H.Y., Luo, Y.L., Li, Y.C., Li, C.H., Seppä, H., 2014. Human influence as a potential source of bias in pollen-based quantitative climate reconstructions. Quat. Sci. Rev. 99, 112–121. https://doi.org/10.1016/j.quascirev.2014.06.005.

Li, M.Y., Xu, Q.H., Zhang, S.R., Li, Y.C., Ding, W., Li, J.Y., 2015. Indicator pollen taxa of human-induced and natural vegetation in Northern China. Holocene 25, 686–701. https://doi.org/10.1177/0959683614566219.

Liu, H.X., Gao, C.Y., Wang, G.P., 2018. Understand the resilience and regime shift of the wetland ecosystem after human disturbances. Sci. Total Environ. 643, 1031–1040. https://doi.org/10.1016/j.scitotenv.2018.06.276.

Liu, H.X., Yu, Z.C., Han, D.X., Gao, C.Y., Yu, X.F., Wang, G.P., 2019. Temperature influence on peatland carbon accumulation over the last century in Northeast China. Clim. Dyn., 1–13 https://doi.org/10.1007/s00382-019-04813-1.

Lu, H.Y., Wu, N.Q., Liu, K.B., Zhu, L.P., Yang, X.D., Yao, T.D., Wang, L., Li, Q., Liu, X.Q., Shen, C.M., Li, X.Q., Tong, G.B., Jiang, H., 2011. Modern pollen distributions in Qinghai-Tibetan Plateau and the development of transfer functions for reconstructing Holocene environmental changes. Quat. Sci. Rev. 30, 947–966. https://doi.org/10.1016/j.quascirev.2011.01.008.

Luo, C.X., Zheng, Z., Tarasov, P., Nakagawa, T., Pan, A.D., Xu, Q.H., Lu, H.Y., Huang, K.Y., 2010. A potential of pollen-based climate reconstruction using a modern pollen-climate dataset from arid northern and western China. Rev. Palaeobot. Palynol. 160, 111–125. https://doi.org/10.1016/j.revpalbo.2010.01.003.

Ma, Y.Z., Liu, K.B., Feng, Z.D., Sang, Y.L., Wang, W., Sun, A.Z., 2008. A survey of modern pollen and vegetation along a south-north transect in Mongolia. J. Biogeogr. 35, 1512–1532. https://doi.org/10.1111/j.1365-2699.2007.01871.x.

Ma, Q.F., Zhu, L.P., Lu, X.M., Wang, Y., Guo, Y., Wang, J.B., Tang, L., 2017. Modern pollen assemblages from surface lake sediments and their environmental implications on the southwestern Tibetan Plateau. Boreas 46, 242–253. https://doi.org/10.1111/bor.12201.

Melles, M., Svendsen, J.I., Fedorov, G., Wagner, B., 2019. Northern Eurasian lakes-late Quaternary glaciation and climate history-introduction. Boreas 48, 269–272. https://doi.org/10.1111/bor.12395.

Qin, F., Zhao, Y., Li, Q., Cai, M.T., 2015. Modern pollen assemblages from surface lake sediments in northwestern China and their importance as indicators of vegetation and climate. Sci. China Earth Sci. 58, 1643–1655. https://doi.org/10.1007/s11430-015-5111-9.

Sun, X.J., Luo, Y.L., Wu, Y.S., 2003. Pollen record of surface sediments from vertical forest zones of Changbai mountain, Northeast China and their relations to the modern vegetation. Acta Bot. Sin. 45, 910–916. https://doi.org/10.1002/cbic.200300593.

Tang, L.Y., Mao, L.M., Shu, J.W., Li, C.H., Shen, C.M., Zhou, Z.Z., 2016. An Illustrated Handbook of Quaternary Pollen and Spores in China. Science Press, Beijing (In Chinese).

Ter Braak, C.J.F., Juggins, S., 1993. Weighted averaging partial least squares regression (WA-PLS): an improved method for reconstructing environmental variables from species assemblages. Hydrobiologia 269/270, 485–502. https://doi.org/10.1007/BF00028046.

Ter Braak, C.J.F., Smilauer, P., 2003. CANOCO Reference Manual and CanoDraw for Windows User's Guide: Software for Canonical Community Ordination (Version 4.5). Microcomputer Power, Ithaca, NY.

Wang, F.X., Qian, N.F., Zhang, Y.L., Yang, H.Q., 1995. Pollen Flora of China. Science Press, Beijing (In Chinese).

Wei, H.C., Zhao, Y., 2016. Surface pollen and its relationships with modern vegetation and climate in the Tianshan Mountains, northwestern China. Veg. Hist. Archaeobot. 25, 19–27. https://doi.org/10.1007/s00334-015-0530-2.

Wei, H.C., Ma, H.Z., Zheng, Z., Pan, A.D., Huang, K.Y., 2011. Modern pollen assemblages of surface samples and their relationships to vegetation and climate in the northeastern Qinghai-Tibetan Plateau, China. Rev. Palaeobot. Palynol. 163, 237–246. https://doi.org/10.1016/j.revpalbo.2010.10.011.

Xing, W., Bao, K.S., Gallego-Sala, A.V., Charman, D.J., Zhang, Z.Q., Gao, C.Y., Lu, X.G., Wang, G.P., 2015. Climate controls on carbon accumulation in peatlands of Northeast China. Quat. Sci. Rev. 115, 78–88. https://doi.org/10.1016/j.quascirev.2015.03.005.

Xing, W., Guo, W.Y., Liang, H.W., Li, X., Wang, C.L., He, J.B., Lu, X.G., Wang, G.P., 2016. Holocene peatland initiation and carbon storage in temperate peatlands of the Sanjiang Plain, Northeast China. Holocene 26, 70–79. https://doi.org/10.1177/0959683615596824.

Xu, Q.H., Li, Y.C., Zhou, L.P., Li, Y.Y., Zhang, Z.Q., Lin, F.Y., 2007. Pollen flux and vertical dispersion in coniferous and deciduous broadleaved mixed forest in the Changbai Mountains. Chin. Sci. Bull. 52, 1540–1544. https://doi.org/10.1007/s11434-007-0187-z.

Xu, Q.H., Li, Y.C., Tian, F., Cao, X.Y., Yang, X.L., 2009. Pollen assemblages of Tauber traps and surface soil samples in steppe areas of China and their relationships with vegetation and climate. Rev. Palaeobot. Palynol. 153, 86–101. https://doi.org/10.1016/j.revpalbo.2008.07.003.

Xu, Q.H., Li, Y.C., Bunting, M.J., Tian, F., Liu, J.S., 2010. The effects of training set selection on the relationship between pollen assemblages and climate parameters: implications for reconstructing past climate. Palaeogeogr. Palaeoclimatol. Palaeoecol. 289, 123–133. https://doi.org/10.1016/j.palaeo.2010.02.024.

Zhang, Y., Kong, Z.C., Wang, G.H., Ni, J., 2010. Anthropogenic and climatic impacts on surface pollen assemblages along a precipitation gradient in north-eastern China. Glob. Ecol. Biogeogr. 19, 621–631. https://doi.org/10.1111/j.1466-8238.2010.00534.x.

Zhang, H., Zhang, Y., Kong, Z.C., Yang, Z.J., Li, Y.M., Tarasov, P.E., 2015. Late Holocene climate change and anthropogenic activities in north Xinjiang: evidence from a peatland archive, the Caotanhu wetland. Holocene 25, 323–332. https://doi.org/10.1177/0959683614558646.

Zhang, Y., Kong, Z.C., Yang, Z.J., 2016. Pollen-based reconstructions of Late Holocene climate on the southern slopes of the central Tianshan Mountains, Xinjiang, NW China. Int. J. Climatol. 37, 1814–1823. https://doi.org/10.1002/joc.4814.

Zhang, Y.J., Duo, L., Pang, Y.Z., Felde, V.A., Birks, H.H., Birks, H.J.B., 2018. Modern pollen assemblages and their relationships to vegetation and climate in the Lhasa Valley, Tibetan Plateau, China. Quat. Int. 467, 210–221. https://doi.org/10.1016/j.quaint.2018.01.040.

Zhao, Y., Yu, Z.C., Liu, X.J., Zhao, C., Chen, F.H., Zhang, K., 2010. Late Holocene vegetation and climate oscillations in the Qaidam Basin of the northeastern Tibetan Plateau. Quat. Res. 73, 59–69. https://doi.org/10.1016/j.yqres.2008.11.007.

Zhao, Y., Li, F.R., Hou, Y.T., Sun, J.H., Zhao, W.W., Tang, Y., Li, H., 2012. Surface pollen and its relationships with modern vegetation and climate on the Loess Plateau and surrounding deserts in China. Rev. Palaeobot. Palynol. 181, 47–53. https://doi.org/10.1016/j.revpalbo.2012.05.007.